Stratospheric ClO and ozone from the Microwave Limb Sounder on the Upper Atmosphere Research Satellite

J. W. Waters, L. Froidevaux, W. G. Read, G. L. Manney, L. S. Elson, D. A. Flower, R. F. Jarnot & R. S. Harwood*

Jet Propulsion Laboratory, California Institute of Technology, Pasadena, California 91109, USA
* Department of Meteorology, Edinburgh University, Edinburgh EH9 3JZ, UK

Concentrations of atmospheric ozone and of ClO (the predominant form of reactive chlorine responsible for stratospheric ozone depletion) are reported for both the Arctic and Antarctic winters of the past 18 months. Chlorine in the lower stratosphere was almost completely converted to chemically reactive forms in both the northern and southern polar winter vortices. This occurred in the south long before the development of the Antarctic ozone hole, suggesting that ozone loss can be masked by influx of ozone-rich air.

THE conversion of anthropogenic chlorine in the stratosphere to chemically reactive forms that deplete ozone[1] has been of increased concern since the discovery[2] of large springtime ozone loss over Antarctica, and findings[3,4] that the loss is due to chlorine chemistry. Heterogeneous chemistry on polar stratospheric clouds (PSCs) followed by the action of sunlight converts stratospheric chlorine from fairly inert to very reactive forms, ClO being dominant[5-7]. Enhanced ClO has been observed to precede the Antarctic ozone loss, with correlation between high ClO and low ozone developing in mid-September[4]. Enhanced ClO in the Arctic has also been observed[8] and associated ozone loss detected[9]. Downward ozone trends at all latitudes outside the tropics have been detected in all seasons[10].

The Microwave Limb Sounder (MLS), launched on 12 September 1991 on the Upper Atmosphere Research Satellite (UARS)[11], is obtaining global measurements of ClO. Ozone, H_2O, temperature and pressure are simultaneously measured. MLS is the first use of microwave limb sounding[12] from a satellite, and here we report the main results for ClO and ozone obtained so far. These results show that in the north, as in the south, the existing chlorine in the lower stratosphere can be virtually completely converted to reactive forms throughout the polar winter vortex. The period of enhanced ClO in the 1991-92 northern vortex, and consequent destruction of ozone, was limited by the lower-stratosphere warming above the PSC threshold in late January, before the longer duration of high-latitude sunlight needed to sustain the ozone destruction cycle. A vortex-integrated ozone loss of ~4% in a lower-stratospheric layer during 1-13 January is calculated from the observed ClO. Measurements of ClO in the south during early and mid-winter have now been made by MLS, and show that ClO within the southern winter polar vortex was enhanced by 1 June 1992, long before the 'springtime' Antarctic ozone hole. A decrease of ozone coinciding with the largest ClO abundances was observed starting in mid-August, and MLS maps have now shown the full extent of coincidence between enhanced ClO and depleted ozone in the Antarctic in late September. Measurements in both hemispheres indicate the difficulty of directly observing ozone loss associated with enhanced ClO in early and mid-winter when an influx of ozone-rich air can be simultaneous with the conversion of chlorine to reactive forms. The presence of enhanced ClO coincident with increasing ozone within the polar vortices implies more overall chemical loss than would be suggested from just the late winter and early spring decrease in Antarctic ozone. This raises the question of the extent to which the implied additional loss is distributed as a longer-term (and perhaps more widespread) ozone reduction. Early 1993 results for the north, when stratospheric temperatures were below the PSC threshold until at least late February, show enhanced ClO for much longer than in 1992, and lower values of late winter ozone abundances throughout most of the Northern Hemisphere. The overall results obtained during the first 18 months of MLS operation indicate that chlorine depletion of stratospheric ozone is of greater concern than previously thought.

The UARS Microwave Limb Sounder

The instrument[13] has three radiometers simultaneously measuring millimetre-wavelength thermal emission in spectral bands near 205 GHz (for ClO, ozone, SO_2 and upper tropospheric H_2O), 183 GHz (H_2O and ozone) and 63 GHz (temperature and pressure). Measurement coverage is from 80° on one side of the Equator to 34° on the other. There are 15 orbits per day, and the orbit plane precesses slowly with respect to the Sun-Earth direction, so that local solar time of MLS measurements at a given latitude (on either the 'day' or 'night' side of the orbit) varies by only 20 minutes during a 24-hour period. UARS performs a 180° 'yaw manoeuvre' when the orbit precesses through 180° (10 times per year), so MLS high-latitude coverage switches between north and south every ~36 days.

Measurements are made continuously day and night, and are not degraded by stratospheric clouds or aerosols. The composition measurements are fairly insensitive to variations or uncertainties in atmospheric temperature. Overall calibration accuracy[14] is ~3%, and radiometric calibration is done on each limb scan by observing an ambient black-body target and cold space. Figure 1 shows examples of measured ClO spectra. Spectra from the upper stratosphere (Fig. 1*a*, *b*) show excellent agreement between balloon and UARS MLS measurements made at the same latitude and season. Spectra from the lower stratosphere (Fig. 1*c*, *d*) indicate comparable ClO abundances over Antarctica on 21 September 1991 and over Moscow on 11 January 1992.

Vertical profiles of atmospheric parameters are retrieved using optimal sequential estimation[15] on spectra from each 65-s limb scan, with no retrieval 'memory' between different scans. Figure 2 shows averages of retrieved ClO profiles for three periods in the 1991-92 Northern Hemisphere winter. Large abundances of lower-stratospheric ClO are evident at high latitudes during January. These enhanced ClO abundances can only be explained by heterogeneous chemistry, and can cause significant ozone

depletion[7]. The 30–40° N lower-stratospheric ClO abundances shown in Fig. 2 agree better with models[16–18] that include sulphate aerosol chemistry[19] than with those containing only gas-phase chemistry, as has also been found[20] by aircraft measurements at these latitudes. Although the ClO increase expected from sulphate aerosol chemistry is too small, ~0.1–0.2 p.p.b.v. (parts per 10^9), to be seen in MLS individual profile measurements, zonal averages of the data over a range of latitudes and seasons will provide valuable information for improving our understanding of this chemistry and its global implications. The upper-stratospheric ClO peak abundances around 2–5 hPa agree well with recent balloon measurements at submillimetre wavelengths[21].

ClO in the 1991–92 northern winter

MLS daily maps showed enhanced localized ClO abundances greater than ~1 p.p.b.v. in the north starting around 14 December 1991. These occurred on the northern edge of daylight measurements near 30° E, 60° N (northern Russia). National Meteorological Center (NMC) data show temperatures below 195 K (roughly the threshold for type-I nitric acid trihydrate PSCs[22,23]) north of this region for several days previously, and indicate southward advection of air into the area where higher concentrations of ClO were observed. By early January 1992, the enhanced ClO had become comparable, both in magnitude and areal extent, to that measured by MLS late September 1991 in the Antarctic ozone hole. Figure 3 shows lower-stratospheric ClO and ozone extracted from the retrieved profiles for 11 January 1992, and mapped on the 465 K potential temperature (θ) surface. Adiabatic flow occurs on constant θ, and atmospheric pressure at $\theta = 465$ K on this day varied between ~45–65 hPa in the Arctic vortex (see below) to ~75–85 hPa in the Aleutian high. The maps were generated using Fourier transform techniques to help to separate temporal and spatial variations[24,25]. Accuracies of ~0.4 p.p.b.v. for ClO and ~0.3 p.p.m.v. (parts per 10^6) for ozone are expected for the maps shown here. MLS data from only the south-going 'day' side of the orbit, where measurement local times varied from 10:30 a.m. at 70° N, to 12:30 p.m. at 40° N, were used (the 'night' side of the orbit shows much smaller ClO abundances, as expected because there is no photolysis of the ClOOCl formed when two ClO molecules combine). United States and European Arctic measurement campaigns have also found high ClO in the 1991–92 northern winter (personal communications from campaign members).

Figure 3 also shows 11 January 1992 maps of temperature, Rossby–Ertel potential vorticity (Q) and winds produced from NMC data. Intersections of Q and θ mark material lines for adiabatic frictionless fluid flow and provide useful diagnoses of the material field evolution[26]. Strong Q gradients bound the vortex that dominates high-latitude winter stratospheric circulation[26], and maps of Q on isentropic (constant θ) surfaces, as in Fig. 3, help to identify the vortex location and structure. Geopotential height and temperature fields produced operationally by NMC are routinely used to calculate Q on isentropic surfaces for daily comparison with MLS maps. The horizontal wind field is estimated using a primitive equation balance, neglecting time tendency and vertical advection terms[27], with the calculation done on the NMC polar stereographic grid. The winds and temperatures are interpolated by a cubic spline from standard NMC pressure levels to the isentropic surfaces on which Q is calculated. Q was also calculated using data from the UK Meteorological Office assimilation system[28]; this agreed in all general characteristics with that calculated from NMC data for this period.

The enhanced ClO is generally bounded on the north by the edge of daylight, and on the south by $Q \approx 2.5 \times 10^{-5}$ K m^2 kg^{-1} s^{-1}. Note the displacement of the vortex and enhanced ClO away from the pole towards Russia, the arm extending over Britain, and longitudinal variations inside the vortex. (The patches of enhanced ClO seen at mid-latitudes are under investigation; instrument noise can produce occasional spurious values of their magnitude.) Minimum temperatures occur over northern Scandinavia, where ClO increases and coincident measurements by the UARS CLAES and ISAMS infrared instruments show the greatest density of PSCs. The sharp ClO increase from night to day and the further increase in the PSC region over Scandinavia seem generally consistent with current understanding[7] of the diurnal chemistry and PSC activation of chlorine. The ClO decrease within the vortex away from the PSC region is correlated with northward excursion of Q contours, indicating air movement to lower solar illumination which would cause less ClOOCl photolysis and ClO. ClO decrease could also be caused by chemical conversion of reactive chlorine back to reservoir forms. NO_2 rapidly reacts with ClO to form $ClONO_2$ (time constant of ~10 minutes at 50 hPa and 195 K for 1 p.p.b.v. each of NO_2 and ClO), and can be produced by photolysis[29] of HNO_3 from evaporating PSC. Q contours coincident with high ClO enter the polar night at ~210 K temperature near ~120–150° E, where 0.7 p.p.b.v. ClO is observed

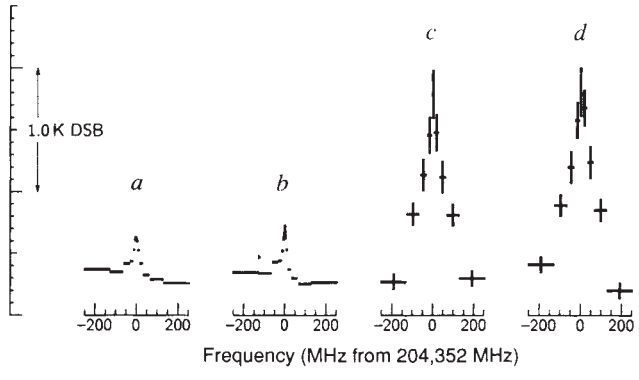

FIG. 1 ClO thermal emission spectra. *a*, Measured by the balloon MLS on 26 September 1989 for 34° N, 33–34 km tangent height and 20 minutes integration time (R. A. Stachnik, personal communication); *b*, average of measurements by UARS MLS on 21 September 1991 at 20–34° N latitudes and 30–40 km tangent height with 3 minutes integration; *c*, measured 21 September 1991 with 1.8-s integration over the Antarctic Weddell Sea at 20 km tangent height—the spectral line is broader than in *a* and *b* because of larger pressure broadening at the lower heights; *d*, measured 11 January 1992 with 1.8-s integration over Moscow at 20 km tangent height. The vertical axis is the emission brightness temperature in 'double-sideband' Kelvin units. Vertical extents of the crosses show $\pm 1\sigma$ measurement noise; horizontal extents show spectral resolution. Some central spectral channels have been averaged together in *c* and *d*. UARS MLS measures spectral points simultaneously in 90 spectral channels, of which only the 15 channels covering ClO are shown here. Its field of view (FOV) is step-scanned through the atmospheric limb between tangent heights of 95 and 5 km every 65 s, during which UARS moves 4° along the orbit. Measurements occur at 1.8-s dwells between steps, and the step spacing varies from 1 km in the lower stratosphere to 5 km in the mesosphere. The FOV vertical extent at the tangent point for the 205-GHz ClO and ozone measurements is 3.5 km, the approximate vertical resolution. Horizontal resolution is ~400 km, set by the distance through the limb where most of the signal originates, and by orbital motion smearing during the limb scan.

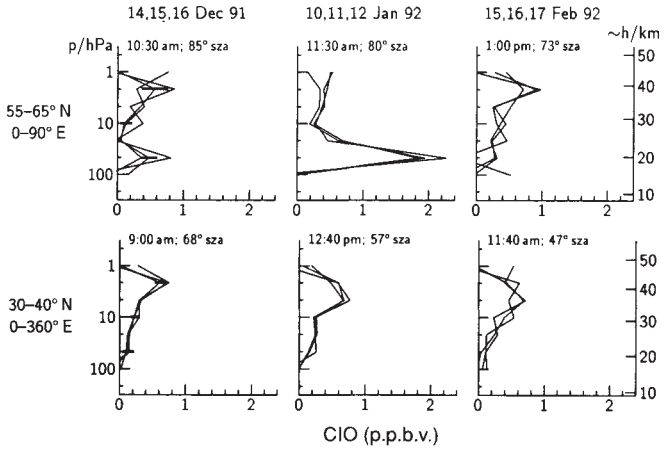

FIG. 2 ClO vertical profiles from UARS MLS. Each panel shows averages over the latitudes and longitudes indicated to the left, for each of the three days indicated at the top; ~12 individual profiles have been averaged for the 55–65° bins, and ~44 for 30–40°. Measurement local solar times and solar zenith angles (sza) for the middle day and the centre of the latitude bands are indicated. Horizontal bars in the left panels give $\pm 1\sigma$ estimated precision in the averaged profiles; absolute accuracy of ~15% is expected. Differences between day and night retrievals have been taken in the 30–40° averages for pressure $p \geq 10$ hPa to remove residual (~0.2 p.p.b.v.) systematic errors. Vertical variation is represented as piecewise-linear in logarithm of atmospheric pressure, with breakpoints at $10^{(6-n)/3}$ hPa, where $n = 0, 1, 2, \ldots$, for the results reported here. Values at the breakpoints are retrieved from MLS spectral measurements taken over each complete limb scan. Approximate heights are indicated on the right.

well into darkness; less than 0.3 p.p.b.v. ClO is observed on these Q contours at ~195 K temperature in darkness near 0° longitude. This night-time ClO variation can be explained by a temperature dependence of ClOOCl thermal decomposition: kinetics data[30] lead to night-time equilibrium ClO values of 0.7 p.p.b.v. at 210 K and 0.15 p.p.b.v. at 195 K, for 2 p.p.b.v. total chlorine in ClO and ClOOCl at 50 hPa. Three-dimensional numerical model results for this period[31,32] provide a more quantitative explanation of the ClO distribution seen by MLS.

Total chlorine in ClO and ClOOCl ($Cl^* \stackrel{def}{=} ClO + 2 \times ClOOCl$, not expected to have significant diurnal variation) can be inferred[33] from ClO. We have done this for the measured ClO and coincident temperature and solar illumination (including calculated attenuation by the measured ozone, and calculated ClOOCl thermal dissociation). ClO abundances greater than ~2 p.p.b.v. at 46 hPa, using nominal values[30] for kinetics parameters and ClOOCl cross-sections, lead to Cl* amounts larger than the ~3 p.p.b.v. inorganic chlorine in the stratosphere[21] available for conversion to ClO. (Total atmospheric chlorine is now at 3.6 p.p.b.v., six times the natural abundance[34].) MLS observations in both north and south have yielded 46 hPa ClO abundances of 2–2.5 p.p.b.v., indicating virtually complete conversion of stratospheric chlorine to reactive forms, but (because of the large values of inferred Cl*) perhaps raising questions concerning details of currently predicted ClO–ClOOCl partitioning and ozone loss calculated from ClO. Further investigations of the large ClO values, and their implications, are in progress.

Figure 4 shows evolution of enhanced ClO on the 465 K isentropic surface during 2–13 January, the last 12 days before switch to south-viewing. The general increase seen in ClO during this period is expected because of increased ClOOCl photolysis as the vortex edge moves to lower latitudes and the rising sun (at 60°, for example, the solar elevation angle at measurement locations increased from 2° on 2 January to 8° on 13 January, while the local time decreased from 2:30 pm to 10:30 am). The

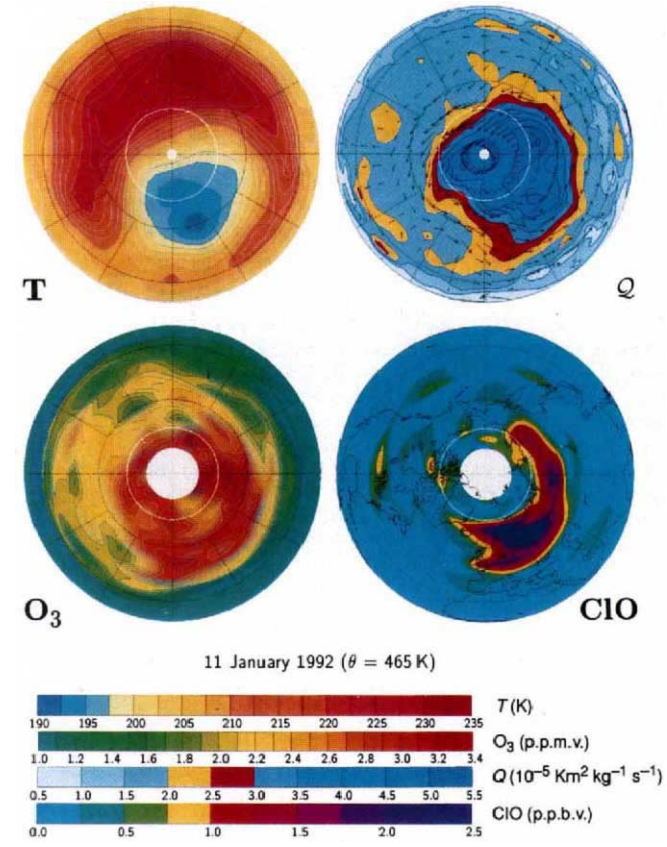

FIG. 3 The 11 January 1992 distribution of Northern Hemisphere ClO, temperature (T), ozone (O_3), and potential vorticity (Q) on the 465 K potential temperature (θ) surface. ClO and O_3 are from UARS MLS, T is from the United States National Meteorological Center (NMC), and Q is calculated from the NMC temperature and geopotential height fields. The Q map also contains calculated wind vectors whose lengths are proportional to wind speed (largest speeds are ~45 m s^{-1}, occurring near the vortex boundary). Values of Q characteristic of the vortex boundary are in red, and values of T for which type-I PSCs can form are in blue. These maps are polar orthographic projections extending outward to the Equator; thin dashed circles are at 30° and 60° latitudes, and land boundaries are included in the ClO map. Thin white circles near 70° N indicate the polar night terminator, and white areas poleward of 80° on the ozone and ClO maps indicate where no MLS measurements are obtained. Local solar times of the measurements in the ClO and ozone maps are near midday and vary only with latitude.

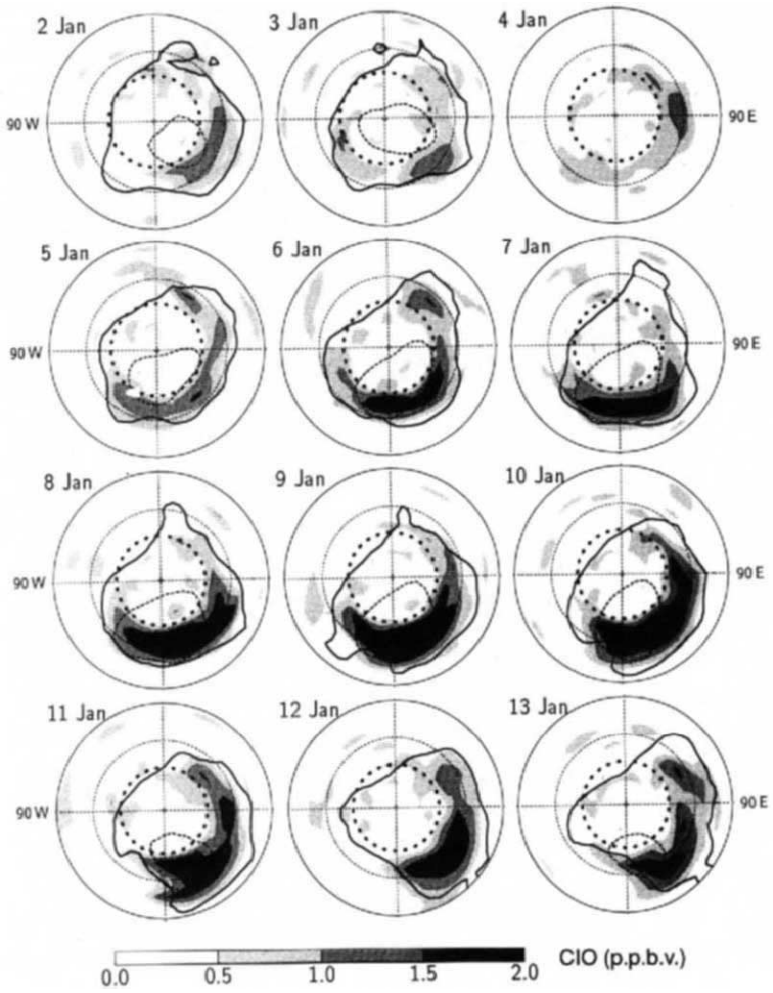

FIG. 4 Variation in the distribution of enhanced ClO during 2–13 January 1992. These maps are polar orthographic projections on the $\theta = 465$ K isentropic surface, like those in Fig. 3, but extend outward to only 40° latitude with 60° latitude indicated by the thin dashed circle. ClO abundance is indicated by the grey scale, the 2.5×10^{-5} K m^2 kg^{-1} s^{-1} potential vorticity contour by the thick solid line, the 195 K temperature contour by the thin (non-circular) dashed line, and the polar night terminator by the thick dashed circle. NMC data, missing for 4 January, showed no temperatures ≤ 195 K on 12 January at $\theta = 465$ K (but did at slightly higher altitudes, for example $\theta = 520$ K).

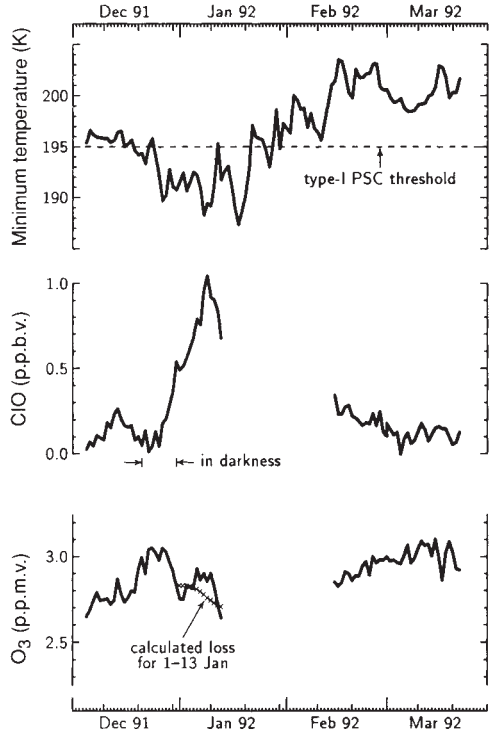

FIG. 5 Temperature, ClO and O_3 in the 1991–92 Northern Hemisphere winter vortex for a lower stratospheric layer at 465 K potential temperature. The vortex boundary is here defined as the 2.5×10^{-5} K m^2 kg^{-1} s^{-1} potential vorticity contour. Minimum temperature is given at the top, with a horizontal line indicating the approximate temperature below which nitric acid trihydrate PSCs form. Average ClO and O_3 mixing ratios, obtained by volume-integrating ClO and O_3 number densities and then dividing by the integrated air in the same volume, are given in the middle and bottom. The volume-integration includes regions of the vortex in daylight and in darkness, and the resulting ClO values are substantially lower than those for just the 'daylight' region. The bottom panel also shows expected ozone evolution with loss calculated from observed ClO and no transport into or out of the layer. Gaps in the ClO and O_3 plots between mid-January and mid-February occur when MLS was south-viewing.

pattern of enhanced ClO tends to move with Q, indicating the importance of atmospheric motions in controlling its distribution. Enhanced ClO is generally contained within $Q = 2.5 \times 10^{-5}$ K m^2 kg^{-1} s^{-1}, but not always (for example, 10 and 13 January, where the 195 K isotherm extended outside $Q = 2.5 \times 10^{-5}$ K m^2 kg^{-1} s^{-1}). Figure 4 shows that air containing large amounts of reactive chlorine can have considerable and variable meridional motion; this strongly affects ozone depletion and must be considered[29] for reliable calculations of ozone loss.

Ozone in the 1991–92 northern winter

The maps in Fig. 3 show correlation between ozone and Q, indicating the importance of atmospheric motions in determining the lower-stratospheric ozone distribution. It also shows that the vortex interior on 11 January contains more ozone at $\theta = 465$ K than the exterior, as expected from the diabatic descent[35] of ozone-rich air from above. The winter evolution of MLS ozone data examined on different θ-surfaces is consistent with ozone-rich mid-stratospheric air moving poleward from lower latitudes and diabatically descending in the vortex. A relative minimum in lower-stratospheric ozone developed in early January near the region of largest ClO, and on 11 January at $\theta = 465$ K (see Fig. 3) amounted to ~15–20% relative to surrounding regions in this layer. Figure 5 shows temperature, ClO and ozone throughout the 1991–92 winter at $\theta = 465$ K within the Arctic vortex. The lower stratosphere was cold enough for type-I PSCs from mid-December through late January. Measured ClO and ozone are shown, integrated throughout the vortex for $Q > 2.5 \times 10^{-5}$ K m^2 kg^{-1} s^{-1} and for a layer bounded by $\theta = 450$ K at the bottom and $\theta = 480$ K at the top (~2.5 km vertical thickness). Vortex-integrated ClO increased greatly in early January, then decreased throughout February and March following the late-January warming above temperatures at which PSCs form. The expected climatological increase in high-latitude winter ozone is evident, but a decrease of ~10% occurs between late December and mid-January. Enhanced ClO was observed by MLS during late December, but these measurements occurred either in darkness or at very low solar zenith angles and an observed midday value was not obtained.

Ozone loss over time Δt due to the ClO+ClO cycle[6,36] is given[37] by $\Delta O_3^c = 2k[ClO]^2[M]\Delta t$ molecule m^{-3}, where k is the rate constant[30] for the ClO+ClO+M reaction, M indicates a third molecule and [X] is number density of species X. Using measured values of [ClO], [M] (obtained from temperature and pressure) and temperature (needed for k), we calculated daily fields of ΔO_3^c for 1–13 January 1992. Diurnal variation was included by inferring Cl* from ClO at each measurement point and integrating the ozone loss (expressed in terms of Cl*) over a diurnal cycle while accounting for varying ClOOCl photolysis due to changing solar zenith angle. Results from such calculations differ negligibly from those obtained by a more accurate time-dependent calculation. Estimated additional loss from the ClO+BrO cycle[38] was included by multiplying the calculated ΔO_3^c by 1.4, appropriate for 8 parts per 10^{12} (p.p.t.v.) BrO (previously measured[39] in the Arctic vortex) and 1.5 p.p.b.v. ClO (typical daytime vortex value from MLS). Localized losses up to ~4% per day were calculated for the 465 K layer during 1–13 January. The fields of calculated ΔO_3^c were volume-integrated in the same manner as the measured ozone and ClO, and the results are given in Fig. 5. We obtain a maximum vortex-integrated loss of ~1% per day for the layer, and 4% cumulative loss over the 13-day period. The measured ozone shows variations (both increases and decreases) larger than the calculated loss, illustrating the difficulty of distinguishing between chemical and dynamical effects on the observed ozone.

Comparison with the 1992 southern winter

In 1992 MLS measured ClO enhanced to >1 p.p.b.v. in the south starting at the beginning of its south-viewing period on 1 June. On this day the vortex was displaced from the pole to the west, and ClO > 1 p.p.b.v. was observed equatorward of 60° S at 10–75° W, reaching 53° S at 60° W (near the Falkland Islands), and bounded on the north by $Q \approx -3.5 \times 10^{-5}$ K m^2 kg^{-1} s^{-1} and on the south by the daylight edge (~65° S) of measurements. NMC data show that the lower stratosphere had already cooled below the ~195 K type-I PSC threshold by 10 May, and OClO measurements[40] at 78° S had previously indicated chlorine activation early in the 1991 southern winter. ClO increased as the winter progressed. By 14 August, when MLS started another south-viewing period, much of the lower stratosphere poleward of 60° S in daylight (equatorward of 78° S) contained ~2–2.5 p.p.b.v. ClO; the distribution at $\theta = 465$ K is shown on the cover. These measurements suggest that the May–August downward decadal trend[10] in southern high-latitude ozone is due to chlorine but, with only one year's measurements, we cannot yet say whether 1992 might have been unusual because of effects of the Pinatubo eruption. OClO measurements indicate increased chlorine activation by sulphate aerosol chemistry in 1992 relative to that before Pinatubo in 1991 (ref. 41). The outer boundary of enhanced ClO (at $\theta = 465$ K) retreated poleward during late winter, to $Q \approx -5 \times 10^{-5}$ K m^2 kg^{-1} s^{-1} by 20 September. Poleward retreat of the ClO boundary is under investigation and could be caused, for example, by NO_2 from the returning Sun's photolysis of HNO_3.

There was a large loss of ozone within the Antarctic vortex in September. Figure 6 shows maps of the vertical columns of ClO and ozone for 20 September 1992, the last day of measurements before the switch to north-viewing. Corresponding maps are shown for 21 September 1991 data obtained shortly after launch. The full extent of correlation between enhanced ClO

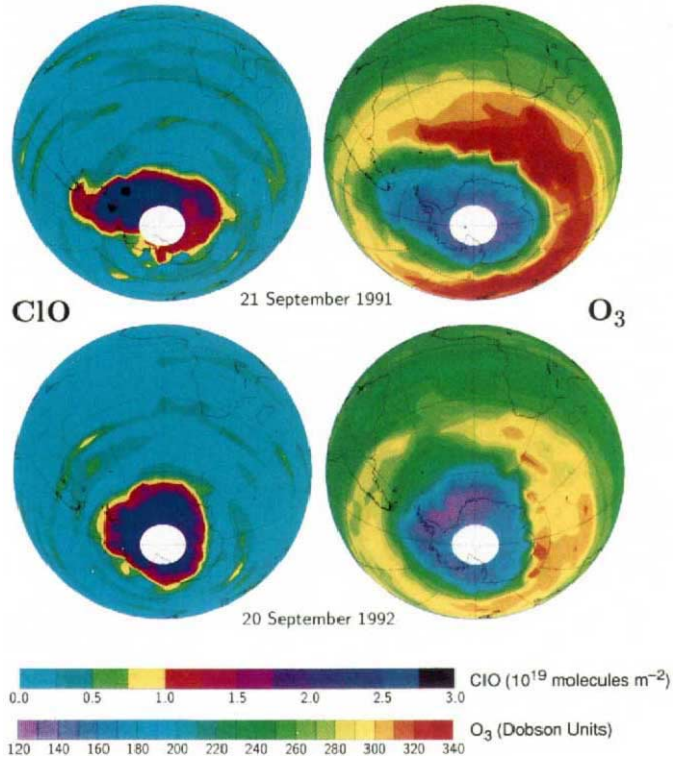

FIG. 6 ClO and O_3 in the Southern Hemisphere on 21 September 1991 and 20 September 1992. The mapped quantities are vertical columns obtained by integrating the profiles retrieved from MLS. The O_3 column is in Dobson units (2.69×10^{20} molecule m^{-2}) above 100 hPa. The patches of ClO outside the vortex are near the noise level. These maps were produced using linear interpolation of measurements, in contrast to those in Fig. 3, which were produced using Fourier techniques.

and depleted ozone is evident. Ozone abundances in the 'collar' around Antarctica were noticeably lower in 1992 than in 1991, and this difference is being investigated. It is informative that largest reduction in vortex ozone did not occur until September, even though greatly enhanced ClO was present from early June, with more in August than in September. This suggests a net flux of ozone into the lower stratosphere during the earlier period to counter chemical loss indicated by the enhanced ClO and, as discussed earlier for the north, our data appear consistent with diabatic descent of ozone-rich air. Continuing studies of both the horizontal and vertical evolution of the measured ozone (and other) fields should help quantify the extent to which the vortex is isolated from or interacts with the outside—crucial for implications of more widespread ozone depletion[42,43].

A major difference between the two hemispheres, with regard to chlorine activation and associated ozone loss, is the amount of time that the stratosphere is sufficiently cold for PSCs: this was ~5 months for the south and ~6 weeks for the north during the 1991–92 winter seasons. A related difference is minimum temperatures. At ~190 K, type-II ice PSCs can form[23] and sediment out of the stratosphere, removing HNO_3 as a source for NO_2 to quench ClO and reduce ozone destruction[44,45] (type-I PSCs can also grow sufficiently large under suitable conditions[44] to sediment and remove HNO_3). Lower-stratospheric temperatures in the Southern Hemisphere were <190 K for ~4 months in 1992, but only occasionally so in the Northern Hemisphere 1991–92 winter. The warmer northern temperatures can be traced to stronger planetary waves resulting from greater orographic and thermal forcing by the more varied northern land distribution[46]. Planetary waves can mix warm air into polar regions and induce adiabatic compression and heating, leading to diabatic cooling that results in descent across isentropic surfaces. However, planetary waves can also displace the vortex from the pole, causing more air to move into sunlight and thus increasing ClO once PSCs have formed; MLS maps have shown that this can be appreciable.

Early results from 1993 and future outlook

Minimum temperatures within the lower-stratospheric Arctic vortex in 1993 remained well below the type-I PSC threshold, and were often below the type-II threshold, until late February. This winter MLS observed ≥1 p.p.b.v. ClO on the $\theta = 465$ K surface from as early as 4 December 1992 (temperatures first dropped below the type-I threshold in late November) to as late as 4 March 1993. The vortex was generally centred nearer the pole in early January 1993 than during the same period in 1992. When MLS north-viewing measurements resumed on 10 February, however, the vortex was displaced from the pole (southward to ~60° N over northeastern Canada and to ~50° N over central Russia), and ≥1 p.p.b.v. ClO was observed throughout most of the vortex at $\theta = 465$ K; the distribution on 14 February is shown on the cover. ClO remained high throughout February, and the vortex continued to be displaced from the pole with minimum lower-stratospheric temperatures below the type-I threshold until at least 25 February. ClO decrease occurred in March, following the late February warming, and the vortex reached as far south as 40° N over the Mediterranean. Vortex-integrated ozone in the 465 K layer decreased by 0.7% per day on average between 10 February and 1 March, whereas during the same period in 1992 (Fig. 5) it increased by 0.3% per day on average. Initial analyses of MLS data show the average ozone column (above ~200 hPa) in late winter throughout most of the extra-tropical Northern Hemisphere to be ~10% lower than in 1992, with regions that are 20% lower. The amount of ozone column decrease in northern winter observed by MLS between 1992 and 1993 is noticeably larger than the <5% winter-to-winter variations seen in the 30-year record of zonally averaged, smoothed Dobson data[47] for the north, and at the extreme of winter-to-winter variations seen in the 10-year record of zonal mean data from the Total Ozone Mapping Spectrometer (TOMS)[47]. Further analyses are under way.

Industrial production of source gases that take chlorine into the stratosphere is decreasing but, even with this positive step towards protecting our ozone shield, anthropogenic chlorine in the stratosphere will continue to increase during the next decade and will be above the abundance at which the Antarctic ozone hole formed for about a century[48]. Additional concerns for stratospheric ozone depletion include the detrimental effects of increasing stratospheric CH_4 (ref. 49), NO_x (ref. 50), aerosols[51] and CO_2 (ref. 52). Fortunately, the technology now exists for continuous global monitoring of both the three-dimensional distribution of stratospheric ozone and processes that can deplete it. □

Received 25 January; accepted 24 March 1993.

1. Molina, M. J. & Rowland, F. S. *Nature* **249,** 810–812 (1974).
2. Farman, J. C., Gardiner, B. G. & Shanklin, J. D. *Nature* **315,** 207–210 (1985).
3. de Zafra, R. L. *et al. Nature* **328,** 408–411 (1987).
4. Anderson, J. G., Brune, W. H. & Proffitt, M. H. *J. geophys. Res.* **94,** 11,465–11,479 (1989).
5. Solomon, S., Garcia, R. R., Rowland, F. S. & Wuebbles, D. J. *Nature* **321,** 755–758 (1986).
6. Molina, M. J., Tso, T. L., Molina, L. T. & Wang, F. C. Y. *Science* **238,** 1253–1257 (1987).
7. Solomon, S. *Nature* **347,** 347–354 (1990).
8. Brune, W. H., Toohey, D. W., Anderson, J. G. & Chan, K. R. *Geophys. Res. Lett.* **17,** 505–508 (1990).
9. Proffitt, M. H. *et al. Nature* **347,** 31–36 (1990).
10. Stolarski, R. *et al. Science* **256,** 342–349 (1992).
11. Reber, C. A. *Trans. Am. geophys. Un.* **71,** No. 51 (December 1990).
12. Waters, J. W. in *Atmospheric Remote Sensing by Microwave Radiometry* (ed Janssen, M. A.) ch. 8 (Wiley, New York, 1993).
13. Barath, F. T. *et al. J. geophys. Res.* (in the press).
14. Jarnot, R. F. & Cofield, R. E. *The Upper Atmosphere Research Satellite (UARS) Microwave Limb Sounder (MLS) Calibration Report, JPL Document D-9393* (Jet Propulsion Laboratory, Pasadena, California, 1991).
15. Rodgers, C. D. *Rev. Geophys. Space Phys.* **14,** 609–624 (1976).
16. Brasseur, G. P., Granier, C. & Walters, S. *Nature* **348,** 626–628 (1990).
17. Rodriguez, J. M., Ko, M. K. W. & Sze, N. D. *Nature* **352,** 134–137 (1991).
18. Brasseur, G. & Granier, C. *Science* **257,** 1239–1242 (1992).
19. Tolbert, M. A., Rossi, M. J. & Golden, D. M. *Geophys. Res. Lett.* **15,** 847–850 (1988).
20. King, J. C. *et al. Geophys. Res. Lett.* **18,** 2273–2276 (1991).
21. Stachnik, R. A., Hardy, J. C., Tarsala, J. A., Waters, J. W. & Erickson, N. R. *Geophys. Res. Lett.* **19,** 1931–1934 (1992).
22. Hanson, D. & Mauersberger, K. *Geophys. Res. Lett.* **15,** 855–858 (1988).
23. McCormick, M. P. *et al. Geophys. Res. Lett.* **17,** 381–383 (1990).
24. Salby, M. L. *J. atmos. Sci.* **39,** 2577–2600 (1982).
25. Lait, L. R. & Stanford, J. L. *J. atmos. Sci.* **45,** 3784–3799 (1988).
26. Clough, S. A., Grahame, N. S. & O'Neill, A. *Q. Jl R. met. Soc.* **111,** 335–358 (1985).
27. Randel, W. J. *J. atmos. Sci.* **44,** 3097–3120 (1987).
28. Swinbank, R. & O'Neill, A. *A Stratosphere–Troposphere Data Assimilation System, Climate Res. Tech. Note* 35 (Hadley Centre for Climate Prediction and Research, Bracknell, 1992).
29. Jones, R. L., McKenna, D. S., Poole, L. R. & Solomon, S. *J. geophys. Res.* **17,** 545–548 (1990).
30. DeMore, W. B. *et al. Chemical Kinetics and Photochemical Data for Use in Stratospheric Modeling: evaluation number 10, Tech. Rep.* 92–20 (Jet Propulsion Laboratory, 1992).
31. Kettleborough, J. *et al. Geophys. Res. Lett* (submitted).
32. Lefèvre, F. *et al. Nature* (submitted).
33. Rodriguez, J. M. *et al. J. geophys. Res.* **94,** 16683–16703 (1989).
34. World Meteorological Organization and United Nations Environment Program, *Scientific Assessment of Stratospheric Ozone, 1991* (WMO Geneva, 1991).
35. Schoeberl, M. R., Lait, L. R., Newman, P. A. & Rosenfield, J. E. *J. geophys. Res.* **97,** 7858–7882 (1992).
36. Molina, L. T. & Molina, M. J. *Phys. Chem.* **91,** 433–436 (1987).
37. Anderson, J. G. *et al. J. geophys. Res.* **94,** 11480–11520 (1989).
38. McElroy, M. B., Salawitch, R. J., Wofsy, S. C. & Logan, J. A. *Nature* **321,** 759–762 (1986).
39. Toohey, D. W., Anderson, J. G., Brune, W. H. & Chan, K. R. *Geophys. Res. Lett.* **17,** 513–516 (1990).
40. Sanders, R. W. *et al. J. geophys. Res.* (in the press).
41. Solomon, S. *et al. Nature* (in the press).
42. Hartmann, D. L., *et al. J. geophys. Res.* **94,** 11625–11640 (1989).
43. Tuck, A. F. *J. geophys. Res.* **94,** 11687–11737 (1989).
44. Toon, O. B., Turco, R. P. & Hamil, P. *Geophys. Res. Lett.* **17,** 445–448 (1990).
45. Wofsy, S. C., Salawitch, R. J., Yatteau, J. H. & McElroy, M. B. *Geophys. Res. Lett.* **17,** 449–452 (1990).
46. Schoeberl, M. R. & Hartmann, D. L. *Science* **251,** 46–52 (1991).
47. World Meteorological Organization *Rep. int. Ozone Trends Panel 1988, WMO Global Ozone Res. Monitoring Proj. Rep. No. 18* (WMO, Geneva, 1988).
48. Benedick, R. E. *Ozone Diplomacy* (Harvard Univ. Press, Cambridge, Massachusetts, 1991).
49. Blake, D. R. & Rowland, F. S. *Science* **239,** 1129–1131 (1988).
50. Johnston, H. S., Kinnison, D. E. & Wuebbles, D. J. *J. geophys. Res.* **94,** 16351–16363 (1989).
51. Hofmann, D. J. *Science* **248,** 996–1000 (1990).
52. Austin, J., Butchart, N. & Shine, K. P. *Nature* **360,** 221–225 (1992).

ACKNOWLEDGEMENTS. We thank many colleagues for contributing to MLS; NASA, the UARS Project and associates for UARS; R. W. Zurek's UARS team (of which G.L.M. is a member) for derived meteorological products; I. MacKenzie for diurnal integrations; W. G. Grose and team for atmospheric model data used in pre-launch simulations; A. J. Miller and A. O'Neill and their teams for meteorological data following launch; the ISAMS and CLAES UARS teams for data on polar stratospheric clouds; P. A. Newman for supplying routines that were adapted to calculate potential vorticity; D. W. Fahey, C. B. Farmer, J. R. Holton, J. A. Pyle, M. R. Schoeberl, A. F. Tuck and R. W. Zurek for comments. The work at JPL Caltech was sponsored by NASA and the work at EU by SERC.